

The chemistry and structure of redledgeite

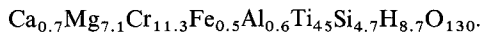
B. M. GATEHOUSE,¹ G. C. JONES,³ A. PRING,² AND R. F. SYMES³

¹Department of Chemistry, Monash University, Clayton, Vic. 3168, Australia. ²South Australian Museum, North Terrace, Adelaide, SA 5000, Australia. ³Department of Mineralogy, British Museum (Natural History), Cromwell Road, London, SW7 5BD, England.

ABSTRACT. Two distinct habits of redledgeite are described: small black bipyramidal crystals and yellow-green fibres. The mineral is a Ba-Cr-Ti oxide rather than a Mg-Cr-Ti oxide as previously supposed. Electron microprobe analysis gave $\text{Ba}_{1.10}(\text{Cr}_{1.82}\text{Ti}_{5.95}\text{Fe}_{0.10}\text{V}_{0.08})_{\Sigma 7.95}\text{O}_{16}$ and $\text{Ba}_{1.27}(\text{Cr}_{2.48}\text{Ti}_{5.49}\text{Fe}_{0.02})_{\Sigma 7.99}\text{O}_{16}$ for the black and yellow-green forms respectively. The mineral is a monoclinic hollandite-type phase, space group $I2/m$, with $a = 10.129(2)$; $b = 2.95(1)$; $c = 10.135(2)$ Å; $\beta = 90.05(11)^\circ$ and $Z = 1$; calculated density for the black form is 4.413 g cm^{-3} . The crystal structure was refined to R 6.3%, R_w 7.4% using 1017 reflections with $F > 3\sigma(F)$ from a set of 1062 unique reflections. Electron diffraction studies revealed weak superlattice reflections, with a period of $2.24b$ due to tunnel cation ordering.

KEYWORDS: redledgeite, crystal chemistry, hollandite-type structure, Red Ledge gold mine, California.

THE rarest and least well characterized of the hollandite-type minerals is redledgeite. Known only from the Red Ledge gold mine, Washington district, Nevada County, California, USA, the mineral is found in close association with kämmererite, $(\text{Mg,Cr})_6(\text{AlSi}_3\text{O}_{10}(\text{OH}))_{10}$ (a chromium chlinochlore) and chromite $(\text{Mg,Fe})\text{Cr}_2\text{O}_4$. Redledgeite was originally described as 'chromrutile' by Gordon and Shannon (1928). Their analysis gave



Strunz (1961, 1963) established that the mineral was structurally related to hollandite rather than rutile, and the mineral was renamed after the type locality. Strunz found the mineral to be tetragonal, space group $I4_1/a$, and noted a strong hollandite-like subcell, $a = 10.10$ and $c = 2.92$ Å. Evidence of a doubling of both the tetragonal a and c repeats was found, and the full cell was determined as $a_0 = 20.32$, $c_0 = 5.84$ Å (Strunz, 1961). He determined the cell contents, based on the original analysis (Gordon and Shannon, 1928), as $\text{MgTi}_6\text{Cr}_{1.5}\text{Si}_{0.5}\text{O}_{16}$ and assigned Mg to the tunnel sites.

There are two chemically distinct groups of hollandite-type minerals: the manganese oxide hollandites, of which cryptomelane, $\text{KMn}_8\text{O}_{16}$,

and hollandite, $\text{BaMn}_8\text{O}_{16}$, are the most common; and the titanium-oxide-based hollandites of which redledgeite is an example. Both groups of minerals share the same distinctive tunnel structure which was originally determined by Byström and Byström (1950) for the mineral hollandite. The structure, as shown in fig. 1, consists of a framework of octahedrally coordinated metal ions. The octahedra are linked by edge-sharing to form double columns parallel to the tunnel axis. The double strings in turn share corners to form a three-dimensional framework containing square tunnels. In the closely related hollandite-type mineral, priderite $(\text{K,Ba})(\text{Fe,Ti})_8\text{O}_{16}$, the large cations, Ba and K, occupy the tunnel sites (Post *et al.*, 1982, and

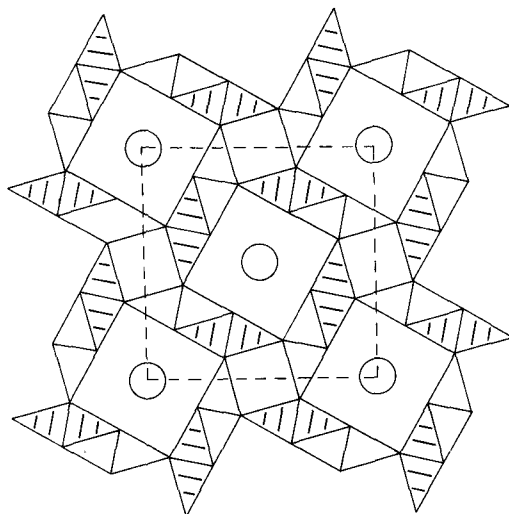


FIG. 1. The idealized tetragonal hollandite structure projected along the tunnel axis [001]. Pairs of edge-sharing octahedra form columns parallel to [001] which in turn share corners to form square tunnels which run through the structure. The larger cations (Ba in the case of redledgeite) shown as circles occupy eight coordinated sites within the tunnels.

Sinclair and McLaughlin, 1982). Since Ba and K are much larger than Mg it was considered unlikely that the structural formula, as proposed by Strunz, could be correct. A re-examination of redledgeite, combining new chemical data from electron microprobe analysis and a structure refinement by single-crystal X-ray diffraction methods, was therefore undertaken.

DESCRIPTION

Redledgeite occurs at the Red Ledge mine in two forms. The mineral was originally found as brilliant black bipyramidal crystals, up to 2 mm in length, on a slightly weathered chromite matrix. Redledgeite also occurs in a dark yellow-green fibrous form which appears not to have been described. A scanning electron microscopic study of the fibrous form revealed tiny prismatic crystals of redledgeite approximately 10 to 15 μm in length and less than 1 μm in diameter (fig. 2), although larger fibres, up to several millimetres, have been found. Both forms

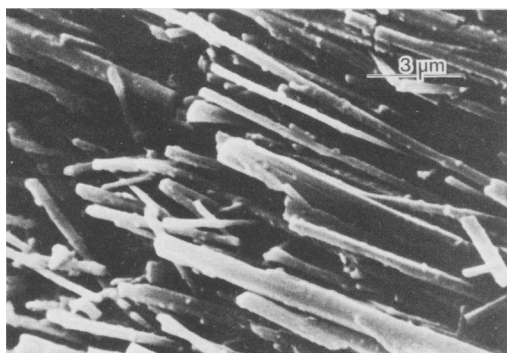


Fig. 2. Scanning electron micrograph of fibrous redledgeite crystals. Individual crystals are approximately 1 μm in diameter and 10–15 μm in length.

occur in association with k ammererite and a chromite matrix. The striking difference in colour between the two forms can be attributed to differences in crystal size and chromium and iron contents as thin fracture fragments of the larger black crystals show dark green edges, and the fibres have a higher Cr and lower Fe content. The chemical data presented in the following section show that the two forms are otherwise chemically very similar. Measurement on the black crystals gave a Mohs hardness of 6.5; it was not possible to determine the hardness of the fibrous crystals.

CHEMICAL ANALYSIS

One small crystal fragment (maximum dimension 300 μm) of type redledgeite (USNM 95846) was

available to us for chemical study, the X-ray diffraction pattern of which was found to be identical to that of black bipyramidal crystals from the redledgeite specimen BM 1928, 336. A polished mount of the type fragment would only take a poor polish but electron microprobe analyses obtained on this were within the elemental range for BM 1928, 336 shown in Table I. Several 30 μm inclusions of k ammererite were found in this type redledgeite fragment. In order to obtain large areas of well-polished crystal section for analysis, several bipyramidal crystals were selected from BM 1928, 336, mounted, polished and analysed. These crystals were found to be homogeneous and free from inclusions.

Preliminary energy dispersive X-ray analysis of the dark yellow-green fibrous form of redledgeite (BM 1973, 575) revealed that Ti, Cr, and Ba were the main chemical constituents, with Mg absent. Subsequent electron microprobe analysis of specimens of both forms confirmed that redledgeite

TABLE I. Electron microprobe analyses of redledgeite

Wt. %	1 Green, fibrous (BM 1973, 575)	2 Black, bipyramidal crystals (BM 1928, 336)
TiO ₂	53.0 (52.2 – 53.4) †(54.2)	58.6 (57.7 – 59.9)
Cr ₂ O ₃	22.8 (22.0 – 23.5) †(21.0)	17.0
*Fe ₂ O ₃	0.2	1.0 (0.7 – 1.4)
V ₂ O ₅	not detected	‡0.7
BaO	23.6 (22.6 – 24.7) †(20.4)	20.8 (19.2 – 23.1)
TOTAL	99.6	98.1

Cell contents per 16 oxygens

Ti	5.49	} 7.98	Ti	5.95	} 7.95
Cr	2.48		Cr	1.82	
Fe	0.02		Fe	0.10	
V	–		V	0.08	
Ba	1.27		Ba	1.10	

* Total iron determined as Fe₂O₃.

1) Average of 4 energy dispersive analyses. † (Figures in brackets – previous analysis on other fibrous areas).

2) Average of 21 wavelength dispersive analyses. ‡ Energy dispersive value (2 analyses).

Material was prepared as polished grain mounts. The majority of analyses were carried out using a Cambridge Instruments Microscan 9 wavelength dispersive instrument and corrected using a standard ZAF program. Analysis conditions were 20kV (2.5 × 10⁻⁸ A) and standards used were baryte, barium fluoride, pure Cr, pure Fe, and synthetic rutile. Further analyses were run on a Cambridge Instruments Geoscan-Link Systems EDS instrument at 15kV (0.5 × 10⁻⁸ A). Analyst G. C. Jones.

is essentially a barium chromium titanate (see Table I). The microprobe analyses gave the formulae $\text{Ba}_{1.27}(\text{Cr}_{2.48}\text{Ti}_{5.49}\text{Fe}_{0.02})\text{O}_{16}$ and $\text{Ba}_{1.10}(\text{Cr}_{1.82}\text{Fe}_{0.10}\text{Ti}_{5.95}\text{V}_{0.08})\text{O}_{16}$ for the fibrous and bipyramidal forms respectively. Trace vanadium was detected and measured in the bipyramidal crystals but was not detected in the fibrous material. The analyses are consistent with the constraints imposed by the nature of the hollandite structure; the number of Cr, Ti and Fe atoms sum to approximately eight, indicating full occupation of the eight octahedral sites within the standard hollandite-type cell, as confirmed by the structure refinement (see following section).

Since experimental details are not available for the original wet chemical analysis of redledgeite by Shannon (Gordon and Shannon, 1928), it is not possible to determine whether Ba could have been wrongly assigned as Mg in the original analysis. The presence of Si, however, indicates that kämmererite $(\text{Mg,Cr})_6(\text{AlSi}_3)\text{O}_{10}(\text{OH})_8$ was present as an impurity. Si, if present in redledgeite, would have to occupy an octahedral site within the framework. This is most unlikely as six coordinated silicon is known only in minerals formed at very high pressure (e.g. stishovite, the rutile-like polymorph of SiO_2). Most of the Mg in the original analysis could therefore be due to the kämmererite impurity.

CRYSTALLOGRAPHY

Electron diffraction

Electron diffraction studies of redledgeite were undertaken in an attempt to confirm the $2a \times 2c$ supercell reported by Strunz (1961). Crystals of both redledgeite forms were examined by electron microscopy using the same experimental procedures as Pring and Jefferson (1983). The basic tetragonal subcell for redledgeite was confirmed by electron diffraction studies but the true symmetry was later shown to be monoclinic (see structure refinement). The monoclinic y axis is parallel with the tunnels, while in tetragonal hollandite the tunnels are parallel with z . Fig. 3 shows an electron diffraction pattern of redledgeite (black crystals) with the beam parallel to $[111]$; the diffuse superlattice reflections at 0.23 reciprocal lattice units from the rows of principal reflections should be noted. These can be interpreted as a superlattice of period $2.24 \times b$ that roughly corresponds to the doubling of the short axis reported by Strunz. No evidence was found of the doubling of the 10 Å axis which was also reported. Twinning on $(110)_{\text{tet}}$ in hollandite-type compounds is quite common [see example in Post *et al.* (1982) and the resulting

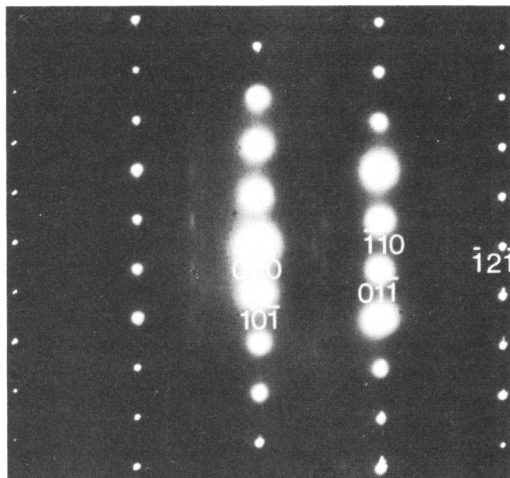


FIG. 3. Electron diffraction pattern produced by a black redledgeite crystal with the beam parallel to $[111]$. Note the incommensurate superlattice reflections with a period of $4.48d_{121}$, $2.24 \times b$ due to the disordered intergrowth of $5b$ body centred supercells with b supercells in the ratio 1:1.

doubling of reflections in the $[110]$ direction could be interpreted as a doubling of a , noting that $(h00)$ with $h \neq 2n$ reflections are absent in body-centred cells].

The origin of superlattice ordering in hollandite-type compounds has been the subject of considerable research during the last few years. Bursill and Grzanic (1980) showed that incommensurate superlattices in tetragonal hollandites, of the type $\text{Ba}_x\text{Al}_{2x}\text{Ti}_{8-2x}\text{O}_{16}$ and $\text{Ba}_x\text{Ga}_{2x}\text{Ti}_{8-2x}\text{O}_{16}$, were due to the disordered intergrowth of $2c$ supercells with supercells of a large period (i.e. $5c$ and $6c$). The supercells are formed by ordering of the large Ba cations in the tunnel sites. Bursill and Grzanic's model for supercell ordering has recently been used to explain superlattice reflections observed in priderite (Pring and Jefferson, 1983), and likewise it can be extended to redledgeite. The observed superlattice corresponds to the disordered intergrowth of $5b$ supercells with $2b$ supercells in a ratio of approximately 1:1. This implies a tunnel stoichiometry of 1.1 Ba atoms per cell, a value in good agreement with the analytical figure. Tunnel cation ordering is discussed later in connection with results of the structure refinement.

Structure refinement

Intensity measurement. Specimens of both forms of the mineral were examined. Because crystals of

the fibrous form were found to be unsuitable for structure determination, a small black crystal fragment was selected for this purpose from the type material (USNM no. 95846). The data crystal, a square based trigonal prism (see below) (0.175 mm high by 0.15 mm on edge) was mounted on a silica-glass capillary and transferred to a Philips PW1100 4-circle automatic diffractometer for intensity measurement. Least squares refinement of 2θ values obtained for centred high-angle reflections gave the pseudo-tetragonal cell $a = 10.129(2)$, $b = 2.951(1)$, $c = 10.135(2)$ Å, but examination of Friedel sets of reflections indicated the true symmetry to be monoclinic with $\beta = 90.05(11)^\circ$. The systematic extinctions were found to be consistent with the space group $C2/m$, but the non-standard setting $I2/m$ was adopted as β is then 90.00° and the structure is easily compared with the tetragonal hollandite phases. Intensity data were collected with graphite monochromated $M\alpha$ - $K\alpha$ radiation ($\lambda = 0.71069$ Å). An ω - 2θ scan, 2θ limits 6 – 60° , was used with a scan speed of $0.04^\circ \text{ sec}^{-1}$. Two background measurements, each for half the scan time, were made at the scan limits. Intensities were processed in the manner described by Fallon and Gatehouse (1980). A quantity of 1105 reflections were measured and reduced to a set of 1062 unique reflections of which 1017 had $F > 3\sigma(F)$ and were used in the final refinement. An absorption correction based on the crystal faces $(\bar{1}01)$, $(10\bar{1})$, $(\bar{2}\bar{1}\bar{2})$, (101) and $(11\bar{2})$ was applied; the maximum and minimum transmission factors were 0.4313 and 0.2947 respectively. Scattering factor curves for Ba, Cr, Ti, and O neutral atoms were those of Cromer and Mann (1968). All computing was carried out on the Monash University Burroughs 6700 computer. The major program used was SHELX76 (Sheldrick, 1976).

Structure solution and refinement. The structure was solved by Patterson methods; Ba was assigned

to the origin and the two metal ion sites were identified. Subsequent difference Fourier syntheses revealed the positions of the oxygen atoms and an additional tunnel site displaced from the origin along the y axis. The positional and isotropic thermal parameters were refined over three cycles of least-squares refinement. The distribution of the Ba ions over the two tunnel sites (0, 0, 0 and 0.0, 0.1405, 0.0) was refined by fixing, in alternate cycles, first the temperature factors and then the occupancy factors. The distribution of Cr and Ti between the two octahedral metal sites was refined but no preferential substitution of Ti by Cr was observed. The oxygen distribution about the two octahedral sites is very similar, further indicating that there is no preferential Cr ordering into one of the octahedral sites.

After three final cycles of refinement, with anisotropic temperature factors, the refinement converged giving $R = 0.063$ $R_w = 0.074$. The final atomic parameters are presented in Table II and selected bond lengths and angles are given in Table III.

DISCUSSION

Redledgeite is the chromium analogue of the minerals priderite-Ba, $\text{BaFe}_2\text{Ti}_6\text{O}_{16}$ (Zhuravkeva *et al.*, 1978), and mannardite, $\text{BaV}_2\text{Ti}_6\text{O}_{16}$ (Scott and Peatfield, 1986). Redledgeite and priderite are closely related crystallographically and have very similar final atomic parameters, bond lengths and angles; however, the slight differences in atomic positions result in redledgeite (monoclinic) possessing lower symmetry than priderite (tetragonal).

Two tunnel sites, both partially occupied, were located in the refinement of redledgeite. The principal site at the origin contains 75% of the Ba ions and the remainder resides in a second site at 0.0, 0.1405, 0.0. One possible explanation for the

TABLE II. List of atomic parameters including equivalent isotropic thermal parameters (with e.s.d.'s)

	x	y	z	Occupancy	$U_{eq}(\text{\AA})^2$
Ba(1)	0.0000	0.0000	0.0000	43.9(3)%	0.0200(10)
Ba(2)	0.0000	0.1405(30)	0.0000	11.1(3)%	0.0100(30)
M(1) (Cr/Ti)	0.1506(1)	0.0000	0.664(1)	100%	0.0068(3)
M(2) (Cr/Ti)	0.3336(1)	0.0000	0.1507(1)	100%	0.0068(3)
O(1)	0.0392(3)	0.0000	0.3346(4)	100%	0.0062(5)
O(2)	0.6657(3)	0.0000	0.0399(4)	100%	0.0065(5)
O(3)	0.2967(3)	0.0000	0.3441(4)	100%	0.0058(5)
O(4)	0.6557(3)	0.0000	0.2969(4)	100%	0.0058(5)

$$U_{eq} = (U_{11}U_{22}U_{33})^{1/3}$$

TABLE III. Selected bond lengths and angles for redledgeite
(with e.s.d.'s)

Ba(1)-O(4) ($\times 4$)	2.984(3) Å		
Ba(1)-O(3) ($\times 4$)	2.986(3)		
Ba(1)-O(2) ($\times 4$)	3.410(2)		
Ba(1)-O(1) ($\times 4$)	3.415(4)		
Ba(2)-O(4) ($\times 2$)	2.802(5)		
Ba(2)-O(3) ($\times 2$)	2.804(5)		
Ba(2)-O(4) ($\times 2$)	3.209(6)		
Ba(2)-O(3) ($\times 2$)	3.211(6)		
Ba(2)-O(2) ($\times 2$)	3.435(4)		
Ba(2)-O(1) ($\times 2$)	3.440(4)		
M(1)-O(1)	1.923(4)		
M(1)-O(2) ($\times 2$)	1.961(2)		
M(1)-O(4) ($\times 2$)	1.982(2)		
M(1)-O(4)	1.997(4)		
M(2)-O(2)	1.932(4)		
M(2)-O(1) ($\times 2$)	1.965(2)		
M(2)-O(3) ($\times 2$)	1.980(2)		
M(2)-O(3)	1.995(4)		
Angles about M(1) octahedra	Angles about M(2) octahedra		
O(1)-M(1)-O(2) ($\times 2$)	94.2(1)	O(2)-M(2)-O(1) ($\times 2$)	94.2(1)
O(1)-M(1)-O(4) ($\times 2$)	91.7(1)	O(2)-M(2)-O(3) ($\times 2$)	91.7(1)
O(2)-M(1)-O(2)	97.6(2)	O(1)-M(2)-O(1)	97.4(2)
O(2)-M(1)-O(4) ($\times 2$)	82.7(1)	O(1)-M(2)-O(3) ($\times 2$)	82.8(1)
O(2)-M(1)-O(4) ($\times 2$)	92.6(1)	O(1)-M(2)-O(3) ($\times 2$)	92.7(1)
O(4)-M(1)-O(4) ($\times 2$)	81.4(1)	O(3)-M(2)-O(3)	96.3(2)
O(4)-M(1)-O(4)	96.2(2)	O(3)-M(2)-O(3) ($\times 2$)	81.3(1)

presence of the second or 'satellite' site is that it represents an artefact associated with the incommensurate superlattice reflections noted in the previous section. However, the position of the site is inconsistent with the observed superlattice period; one would expect an artefact associated with the superlattice to occur at 0.0, 0.1100, 0.0. Since the intensities of these reflections were not included in the refinement, it is unlikely that an artefact would appear. It is more probable that the satellite Ba population is real and associated with cation-cation repulsions when adjacent tunnel sites are occupied. The separation of adjacent sites is 2.951 Å, corresponding to the b repeat; this is close to the ionic diameter of Ba, 2.84 Å, in eight-coordination with oxygen (Shannon and Prewitt, 1969). Strong repulsion between Ba ions in adjacent sites causes displacement from the origin, thus minimizing these interactions. The predicted intergrowth of $5b$ and $2b$ supercells results, on average, in 28.5% of the Ba ions occupying adjacent tunnel sites, a value similar to the occupancy of the satellite site (see fig. 4).

Similar satellite tunnel sites have been reported for priderite (Sinclair and McLaughlin, 1982, and Post *et al.*, 1982) and in the synthetic hollandite phase $\text{BaAl}_2\text{Ti}_6\text{O}_{16}$ (Sinclair *et al.*, 1980). The priderite crystals studied contained both K and Ba tunnel cations and it is argued that the satellite site results from the positioning of the smaller Ba ion close to one end of the site (Sinclair and McLaughlin, 1982, and Post *et al.*, 1982). The assignment of Ba to this site is, however, somewhat ambiguous because the electron densities of the Ba and K fractions are almost equal, both eleven electrons. It is possible that the satellite site in priderite contains mainly Ba due to the high repulsion between Ba ions along the tunnel; however, a sizeable contribution from K ions cannot be ruled out. For the compound $\text{BaAl}_2\text{Ti}_6\text{O}_{16}$, Sinclair *et al.* (1980) invoked cation-cation repulsion to explain the presence of satellite tunnel sites. In the extreme case of $\text{Ba}_{1.33}\text{Cr}_{2.66}\text{Sn}_{5.34}\text{O}_{16}$ all the Ba is located at the displaced site. The

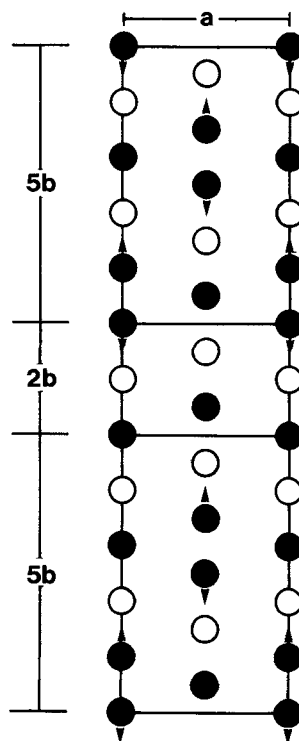


FIG. 4. Schematic diagram of the hollandite structure showing only the sequence of tunnel cation sites in ordered supercells. When adjacent sites are occupied, cation-cation repulsions result in tunnel cation displacement towards the vacant sites (open circles), as indicated by arrow heads.

stoichiometry of this compound is such that two-thirds of the tunnel sites are occupied and thus all Ba cations are paired (Cadée and Verschoor, 1978).

Mannardite, the vanadium analogue of redledgeite, in addition to Ba, contains water within the tunnel sites (Scott and Peatfield, 1986). Lack of material prevented the determination of water in redledgeite. The analytical total for the black form of redledgeite is 1.9% low (Table I). This shortfall, if assigned to water, corresponds to 0.86 H₂O per cell. However, water was not detected during the structure refinement but the possibility that the satellite tunnel site might be due to water was considered. Difference Fourier maps, calculated using only high angle reflections ($2\theta > 40^\circ$), confirmed the Ba occupancy of the satellite tunnel site. At high angles [$(\sin \theta)/\lambda > 0.5$], the scattering power of oxygen declines markedly while that of Ba remains high. If water is present in redledgeite, it will almost certainly occupy the vacant tunnel sites centred on the origin (see fig. 4).

The cause of the small monoclinic distortions observed in many hollandites has been the subject of considerable interest. Sinclair *et al.* (1980) noted a correlation between the size of the octahedrally coordinated cation and the degree of monoclinic distortion; hollandites with larger *M*-type cations tend to be monoclinic. They argued that, as the size of *M* increases, the distortion of the framework octahedra also increases. Post *et al.* (1982) point out that the octahedra in all hollandites are distorted due to edge sharing. They propose, instead, that the monoclinic distortion is related to the displacement of cations from the centre of the octahedra. Displacement along the triad rather than the tetrad axes of the octahedra results in a twisting of the framework and a degeneration of the symmetry. To date, however, neither theory explains comprehensively the observed symmetries for all hollandite-type phases. The monoclinic distortion is often very slight and thus difficult to detect; the cause of the distortion warrants further investigation.

CONCLUSIONS

Analysis of redledgeite has shown that the mineral is a barium chromium titanate and not a magnesium chromium titanate, as previously supposed. Redledgeite is the chromium analogue of priderite-Ba and mannardite.

Redledgeite has a hollandite-type structure but its symmetry is distorted from tetragonal to monoclinic. Ordering of the Ba ions in the tunnels leads to incommensurate 'superlattice' reflections. Supercell ordering reduces the electrostatic interactions between tunnel cations, which are also

reduced by displacing adjacent tunnel cations away from each other along the tunnels.

Acknowledgements. One of us (A.P.) would like to thank Professor J. M. Thomas and Dr D. A. Jefferson for help and encouragement in the initial stages of this work. Dr J. E. Chisholm is thanked for his very constructive comments; Dr John S. White of the Smithsonian Institution, Washington, for provision of a type crystal, and Dr I. E. Grey of CSIRO Mineral Chemistry, Melbourne, for access to his unpublished studies on the mineral. We acknowledge the financial support of the ARGC, AERE Harwell, SERC and the University of Cambridge.

Note. A full listing of structure factors for the redledgeite refinement can be obtained from the Mineral Library of the British Museum (Natural History), Cromwell Road, London SW7 5BD.

ADDENDUM

After this paper was accepted for publication Scott and Peatfield (1986) published a paper describing mannardite (BaV₂Ti₆O₁₆); they also presented a brief redefinition of redledgeite. Their conclusions on the chemistry of this mineral agree with ours but their description of the crystallography of redledgeite differs from that presented here. Scott and Peatfield found a well ordered 2*c* supercell for mannardite; Szymanski (1986) refined the 2*c* superstructure of mannardite in a tetragonal body centred cell $a = 14.356$, $c = 5.911$ Å. Scott and Peatfield found a similar tetragonal cell for redledgeite, i.e. sharp reflections from a dominant 2*c* supercell.

We have not observed these sharp reflections on diffraction patterns such as fig. 3 which would have shown them had they been present. Our results and those of Scott and Peatfield (1986) show that different crystals can have different superlattice periods, probably related to slight differences in stoichiometry. The superlattice period has been shown to vary with stoichiometry in synthetic hollandites (Bursill and Grznic, 1980). In this paper we refined the basic hollandite subcell; the superlattice reflections were too diffuse to be included in the refinement.

REFERENCES

- Bursill, L. A., and Grznic, G. (1980) *Acta Crystallogr.* **B36**, 2902.
 Byström, A., and Byström, A. M. (1950) *Ibid.* **3**, 146.
 Cadée, M. C., and Verschoor, G. C. (1978) *Ibid.* **B34**, 3554.
 Cromer, D. T., and Mann, J. B. (1968) *Ibid.* **A34**, 321.
 Fallon, G. D., and Gatehouse, B. M. (1980) *J. Solid State Chem.* **34**, 1193.
 Gordon, S. G., and Shannon, E. V. (1928) *Am. Mineral.* **13**, 69.
 Post, J. E., Von Dreele, R. B., and Buseck, P. R. (1982) *Acta Crystallogr.* **B38**, 1056.
 Pring, A., and Jefferson, D. J. (1983) *Mineral. Mag.* **47**, 65.
 Scott, J. D., and Peatfield, G. R. (1986) *Can. Mineral.* **24**, 55.
 Shannon, R. D., and Prewitt, C. T. (1969) *Acta Crystallogr.* **B25**, 925.

- Sheldrick, G. M. (1976) SHELX76. Program for crystal structure determination. Cambridge University, England.
- Sinclair, W., and McLaughlin, G. M. (1982) *Acta Crystallogr.* **B38**, 245.
- Ringwood, A. E. (1980) *Ibid.* **B38**, 2913.
- Strunz, M. (1961) *Neues Jahrb. Mineral. Mh.* 107.
- (1963) *Ibid.* 116.
- Szymanski, J. T. (1986) *Can. Mineral.* **24**, 67.
- Zhuravkeva, L. N., Yarkina, K. V., and Ryabera, E. G. (1978) *Dokl. Akad. Nauk SSSR*, **239**, 435.

[Manuscript received 11 October 1985;
revised 25 June 1986]